ISSN 0742-0463, Journal of Volcanology and Seismology, 2007, Vol. 1, No. 2, pp. 98–118. © Pleiades Publishing, Ltd., 2007.
Original Russian Text © S.A. Khubunaya, L.I. Gontovaya, A.V. Sobolev, I.V. Nizkous, 2007, published in Vulkanologiya i Seismologiya, 2007, No. 2, pp. 32–54.

Dedicated to the 100-year anniversary of the birth of Boris Ivanovich Piip

Magma Chambers beneath the Klyuchevskoy Volcanic Group (Kamchatka)

S. A. Khubunaya[a], L. I. Gontovaya[a], A. V. Sobolev[b], and I. V. Nizkous[c]

[a] *Institute of Volcanology and Seismology, Far East Division, Russian Academy of Sciences, Petropavlovsk-Kamchatskii, 683006 Russia*

[b] *Institute of Geochemistry and Analytic Chemistry, Russian Academy of Sciences, Moscow, 111991 Russia*

[c] *Data Services Subsection, Data Consulting and Services Section, Schlumberger Logelco Inc., Moscow, 109147 Russia*

Received November 1, 2006

Abstract—A 3D velocity model of the Earth's crust beneath the Klyuchevskoy volcanic group has been constructed using the seismic tomography method. Anomalies of the velocity parameters related to the zones of magma supply to active volcanoes have been distinguished. Petrological data on the composition, temperature, and pressure of generation and crystallization of parental melts of Klyuchevskoy volcano magnesian basalts have been obtained. The parental melt corresponds to picrite (MgO = 13–14 wt %) with an ultimate saturation of SiO_2 (49–50 wt %), a high H_2O content (2.2–2.9%), and incompatible elements (Sr, Rb, Ba). This melt is formed at pressures of 15–20 kbar and temperatures of 1280–1320°C. Its further crystallization proceeds in intermediate magma chambers at two discrete pressure levels (i.e., greater than 6, and 1–2 kbar). The results of the petrological studies are in good agreement with the seismotomographic model.

DOI: 10.1134/S0742046307020029

INTRODUCTION

The study of the magma chambers beneath the Klyuchevskoy volcanic group (KVG) is one of the relevant problems in volcanology, which is closely related to the problems of geodynamics and eruption prediction. The KVG includes 12 volcanoes and composes a giant rock mass that is located in the northern part of the Central Kamchatka Depression bounded by the Kozyrev–Bystrin system of domes in the west and by the horst-anticlinorium of the Eastern Ranges in the east [17]. A deep magma chamber beneath the Klyuchevskoy Volcano was first distinguished based on the results from upper mantle sounding using P waves induced by tectonic earthquakes [10]. Deep seismic sounding (DSS) of the Earth's crust with the help of explosions [2] in the KVG region was performed in the 1970s. This system of observations made it possible to create a model of the specific features of the crustal seismic boundaries (of the Cretaceous and crystalline basements and Conrad discontinuity). The crust–mantle transition zone (the Moho discontinuity) was studied, primarily using reflected waves, and was characterized by the values of velocities of the strata. In addition to the structural constructions, which were made based on the soundings of the KVG using a single explosion source, we proposed a scheme with a hypothetical magma supply, specifically: we distinguished a magma channel, along which melt comes from the upper mantle to the Klyuchevskoy Volcano crater, and a magma chamber in the middle part of the Earth's crust beneath the Bezymyannyi Volcano related to this magma channel [2]. The following geological–geophysical models of the crust beneath the KVG were principally based the above results [20, 21].

The studies of seismicity registered in this region [10–12, 30–33] considerably contributed to studying the processes that occur beneath volcanoes and which are directly related to the system of magma supply to these volcanoes. In connection with the development of the methods for constructing spatial velocity models, the kinematic parameters of volcanotectonic (VT) earthquakes are widely used to solve structural problems [8, 19]. Gravity field measurements [15] and magnetotelluric sounding [18, 24], which are generally in good agreement with the results of seismic constructions, were also performed in the region of the Klyuchevskoy Volcano.

More detailed seismic studies using the method of refracted waves (MRW) from explosions were performed along a profile crossing the Klyuchevskoy Volcano cone in the 1990s [5]. Based on these data and different interpretation methods, a seismic section of the Earth's upper crust (to a depth of not more than 10 km) was constructed, and anomalies of the P wave velocities (V_p), probably related to the zones of volcano supply, were revealed [5, 23]. However, visible changes in the

P waveforms, which would be observed during seismic sounding of a magma chamber, were not detected (transverse S waves were not registered during the MRW–GSS studies). We assumed that the zone of velocity anomalies is probably related to the presence of a rock sequence, where melt (or fluid) fills small fissures and does not affect the dynamic parameters of seismic waves in a pronounced way, in the crust [5]. It is clear that the depth structure of the KVG is still controversial. At the same time, it is possible to distinguish magma chambers—the regions of magma supply to volcanoes—only by using a complex of geological–geophysical methods, which can present a number of characteristic features indicating that a melt is present in the structure of the Earth's crust.

The monograph *Klyuchevskoy Volcano and Its Eruptions in 1944–1945 and in the Past* by Boris Ivanovich Piip [22] considerably contributed to the study of the mechanism and material composition of KVG eruptions. Piip first assumed that a common magmatic reservoir exists for the volcanoes of the entire Klyuchevskoy group: "… we can assume that a common magmatic reservoir exists for all Klyuchevskoy volcanoes" [22]. Based on the study of xenoliths of the Tertiary rocks from satellite cones lavas on the northeastern flank of the Klyuchevskoy Volcano, Piip showed the existence of intermediate magma chambers [22] at a depth of 5–7 km. Recently, many researchers have paid pronounced attention to the calc–alkaline high-magnesia basalts of the bocche on the northeastern flank of the Klyuchevskoy Volcano, which are unique to island arc systems, and whose composition can be identical to that of mantle [3, 34–36, 46]. Studying the major elements, impurities, and rare earth elements (REEs) of these igneous rocks can make it possible to elucidate the genesis of these rocks and their magma source. Intratelluric phenocrysts of minerals and melt inclusions in these phenocrysts can give fundamental geochemical information about parental melts, the evolution of their compositions, and the physicochemical conditions of magma generation and crystallization [4, 25, 40–42, 50].

In the present paper, we compare the results of the petrological study of magnesian basalts from the Klyuchevskoy Volcano with new data from seismic tomography illustrating the depth velocity structure of the Earth's crust beneath the KVG.

1. METHODS OF STUDIES

Seismic methods. In connection with the development of methods for constructing spatial velocity models, the kinematic parameters of volcanotectonic (VT) earthquakes are widely used to solve structural problems [8, 37]. A seismic tomography method with a high spatial resolution [19] was used to construct a 3D velocity model for the KVG. The calculations were performed using the arrival times of P and S waves induced by VT earthquakes registered at the network of radiotelemetric stations in the KVG region from 2000 to 2004. The catalogs and station data were kindly given by the Kamchatka Branch of the Geophysical Survey of the Russian Academy of Sciences. The times of arrival of seismic waves were interpreted in several main stages, including calculations of the station corrections and optimal 1D velocity model,[1] the repeated determination of hypocenter coordinates (selected from the earthquake catalog) based on this model, estimations of the resolution, and modeling of the spatial velocity model of the Earth's crust. To calculate this model based on the real times of arrival of P and S waves, we selected 11 357 events and 164 196 arrivals including 86 893 P phases and 77 303 S phases.

Seismicity is maximal at depths of 28–37 and 0–3 km. According to the specific location of seismic stations and VT earthquake hypocenters, a relatively reliable model of distribution of P and S wave velocities can be obtained only at depths of 5–30 km. Outside this interval, the velocity parameters may include large errors, and data of other methods (specifically, MRW–GSS) should be taken into account in an analysis of modeling results. We should also note that, according to the results of testing, velocity nonuniformities with intensities lower than ±4% should be ignored since these nonuniformities could be introduced by the computational algorithm and are not related to the velocity structure of the KVG crust. During the calculations, the rms value decreased from 0.40 to 0.24 s. Such a decrease in the rms value means that the major part of the initial error value, related to an insufficiently accurate 1D description of the environment, was corrected by the new and more accurate 3D model.

Methods for studying magnesian basalts. Calc–alkaline magnesian basalts from 21 bocche on the northeastern flank of Klyuchevskoy Volcano have been studied. The monomineral fractions of olivine and pyroxene are described in detail in [35]. The present work uses studies of magmatic inclusions in these minerals, e.g., determination of the phase composition of inclusions and their classification, as well as studies using a quick-response plant operating in a pure helium atmosphere with visual optical control via the Slutskii–Sobolev system [29]. A CAMEBAX electron microprobe at the institute of Volcanology and Seismology, Far East Division of the Russian Academy of Sciences (IViS DVO RAN) was used to study the composition of mineral phases and glass. The analysis was performed at an accelerating voltage of 20 kV and a beam current of 20 nA. The concentrations of the elements were calculated using the MBXCOR program. ISNM 115900 labrador; Ca, blue diopside; Mg and Fe, Fo_{77} olivine; K, sanidine with 12% K_2O; Ti, Mn, and Cr, ilmenite, rhodonite, and chrome-spinel, respec-

[1] The term "optimal" indicates that the 1D model and station corrections give a minimal average rms value of the time of arrival for all earthquakes used in the calculations.

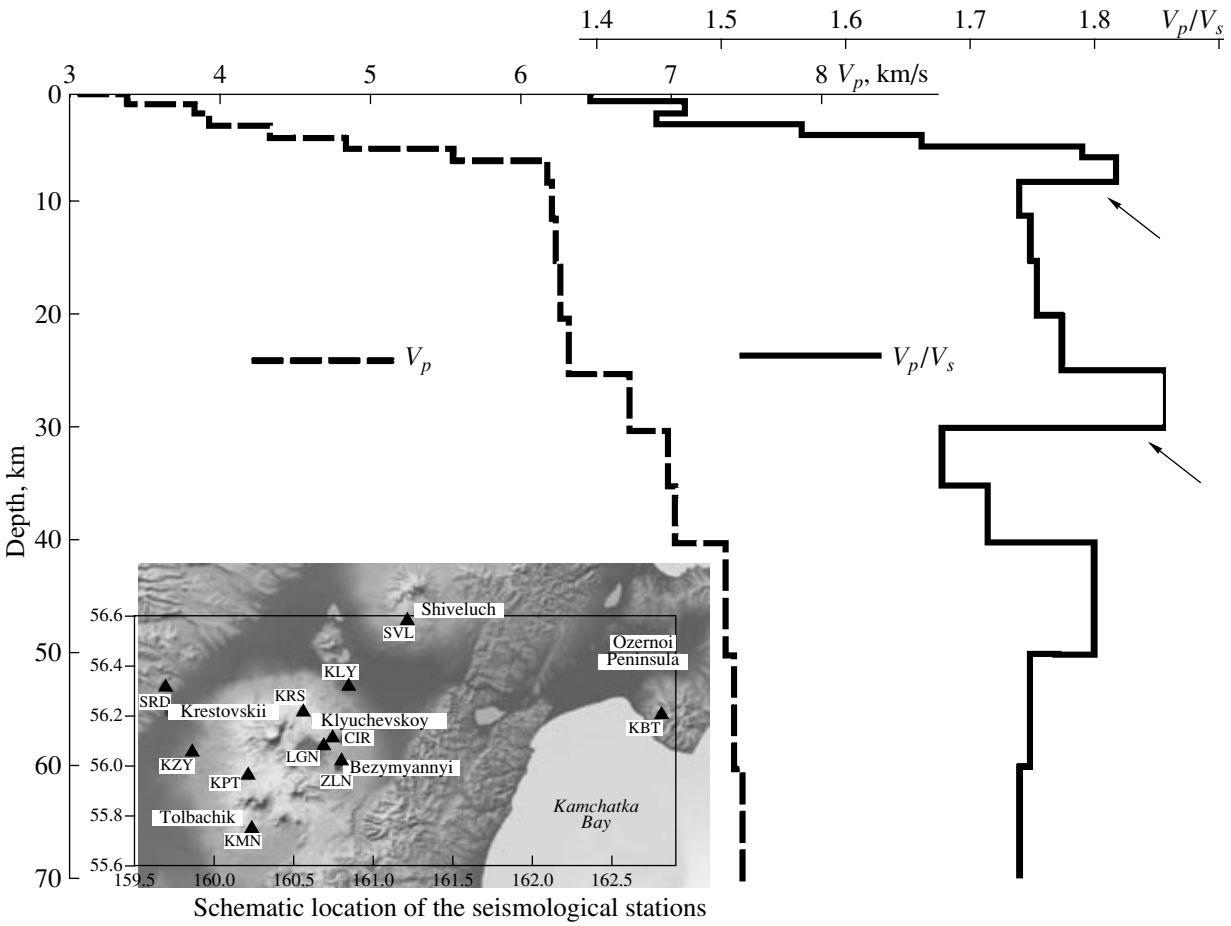

Fig. 1. Average values of the V_p velocity and V_p/V_s parameter for the KVG region. Arrows indicate the layers with anomalously high V_p/V_s values.

tively, were used as standards for determining Si, Al, and Na.

The method of the secondary ion mass spectrometry with a Cameca ims instrument (IM I RAN, Yaroslavl) was used to determine the trace elements and H_2O in glasses of melt inclusions. This technique is described in [25]. The analytical error was 10–15 relative percent at a concentration higher than 1 ppm. The detection limit was 0.01 ppm for trace elements and 0.05 wt % for H_2O.

The major elements and trace elements in the same samples of the representative series of basalts were determined using the method of inductively connected plasma mass spectrometry at the Center of Research in Petrography and Geochemistry (CRPG), Nancy (France) and the method of instrumental neutron activation analysis at the Center of Nuclear Research, Sacle (France). The detection limit was 1 and 20–40 ppb for light and heavy elements-impurities, respectively.

The cryometric studies of fluid inclusions in olivine were performed in a cryogenic camera designed by V.A. Simonov (IGiG SO RAN). The chemistry of the fluid inclusion was determined using Raman scattering spectroscopy (with the use of a MOLE Raman microanalyzer) at the Uranium Geology Research Center, Nancy (France) and also by the J. Dubessy technique [56].

Several calculation methods based on a mineral–melt equilibrium [39] were used to determine the composition of the parental melt of magnesian basalt and the physicochemical conditions of magnesian magma crystallization.

RESULTS OF THE STUDIES AND DISCUSSION

The seismological model of the Earth's crust. The depth velocity structure of the Earth's crust beneath the KVG is characterized by very nonuniform and contrasting anomalies. Even the shape of the curves of the average V_p and V_s velocity values and the V_p/V_s parameter indicates that the crust is highly laminated with respect to its elastic properties (Fig. 1). The V_p/V_s values are increased in the 5–10 and 25–30 km layers and, which is less reliable, at depths of 40–50 km. Anomalies of this parameters are likely caused by weakened fractured zones with melts and (or) fluids.

The results of the calculations with the help of the spatial velocity model of the KVG are presented in the form of horizontal sections, the depths of which coincide with the model layer boundaries, and as vertical sections across the Klyuchevskoy Volcano. The VT earthquakes corresponding to each layer are projected onto the maps of velocity (V_p) anomalies (Fig. 2). In this figure, earthquakes are absent at depths of 0–5 km because only events with $K_s > 5$ are shown in Fig. 2. The interrelation between the seismic character and the velocity anomalies is clearly defined. In the upper portion of the Earth's crust beneath active volcanoes, the velocity is considerably lower (by 15% in comparison to the velocity in the middle crust). The VT earthquakes beneath Klyuchevskoy, Bezymyannyi, and Krestovskii volcanoes, which are probably related to active processes around feeder channels (dikes), are confined to this anomaly. The Klyuchevskoy Volcano cone is located above the central, the lowest-velocity, part of the anomaly; other volcanoes are located at the anomaly periphery. The middle crust beneath the KVG includes a region of increased (by 6–10%) V_p velocity. The VT earthquakes that are not clearly related to specific cones volcanoes are associated with this crust. We can note that these earthquakes are confined to the velocity gradient boundaries within this anomaly, possibly, in the fault zone through which a melt may come from the lower Earth's crust. At depths of 25–30 km a low velocity zone is clearly defined to which all active volcanoes are timed, and Klyuchevskoy Volcano is located at the periphery of this zone in the area of the highest gradients. Deeper (30–35 km), the cone of Klyuchevskoy Volcano is projected onto the center of the anomalous region; all other volcanoes, onto the periphery of this zone.

Figure 3 shows the block scheme of the distribution of the V_p velocity anomalies in the Earth's crust beneath KVG in the form of an intersection of two vertical sections of the 3D volume; the profiles are specified in the NW–SE and SW–NE directions, and Klyuchevskoy Volcano is located in the zone of intersection of these profiles. The contour lines of the V_p velocity absolute values and the hypocenters of all earthquakes, the coordinates of which were repeatedly determined using the calculated velocity model, are also shown on the sections. According to Fig. 3, the depth velocity structure of the upper crust is represented as a flexure filled with a relatively low-velocity sequence. Magmatic melt, which subsequently approaches the surface, likely accumulates at the flexure bottom, and all VT earthquakes are related to this process. The flexure beneath the KVG at the boundaries of the Cretaceous and crystalline basements agrees with the MRW–GSS results [2, 5]. The Krestovskii and Bezymyannyi volcanoes and the lateral cones on the northeastern flank of Klyuchevskoy Volcano are probably located above the fault zones at the periphery of this flexure. The middle part of the Earth's crust includes a high-velocity discontinuity. The central part of the crust is slightly displaced below the northeastern flank of the Klyuchevskoy Volcano. We should note that a high-velocity boundary at a depth of 7–8 km beneath the northeastern flank of Klyuchevskoy Volcano was also distinguished based on the MRW data [23]. Moreover, decreased (to 1.65) values of the V_p/V_s parameter correspond to this region.[2] The region of decreased velocities that is common to all volcanoes in the Klyuchevskoy group is clearly defined in the lower Earth's crust. This anomaly is apparently related to the magma chamber, and the character of seismicity registered in this depth interval reflects the process of travel of a melted mantle material (fluids and melts) through the Earth's crust, which agrees with [12]. The further paths of melts coming to the surface and the possible formation of intermediate chambers are probably both related to the specific structure of the Earth's crust. According to our data, intermediate magma chambers are most probable in the lower and upper parts of the Earth's crust. However, the character of the velocity parameters does not rule out the possibility that these chambers can also be formed in the middle crust (15–20 km), particularly below the Bezymyannyi Volcano. At the present-day level of studies, this problem can be considered only together with data obtained using other geological–geophysical methods during more detailed seismological observations.

The petrological model of magma supply. *Geochemical features of magnesian basalts as indications of basalt generation from one source of magma.* The object of study was the magnesian basalts from the Klyuchevskoy Volcano, the unique igneous rocks of island arcs, the compositions of which may be identical to those of the mantle [3, 34, 35, 46]. Basalts erupted during a prolonged period (from the Early Holocene to the present) on the northeastern flank of the Klyuchevskoy Volcano at heights of 400–1800 m (Fig. 4). The distal portions of the magnesian basalt bocche are located at a distance of 30 km from each other but are, nevertheless, characterized by common mineralogical and geochemical features.

The petrochemical features of magnesian basalts were studied based on the average chemistry of 21 magnesian bocche on the Klyuchevskoy Volcano [35]. According to the K_2O content, these basalts are typical calc–alkaline magnesian rocks. The average compositions of all magnesian and high-alumina basalts from Klyuchevskoy Volcano form a common trend. An increase in MgO in the rock results in an increase in CaO in this rock and in a simultaneous decrease in Al_2O_3, TiO_2, Na_2O, SiO_2, and K_2O. Moreover, the calculated composition of the magnesian basalt, obtained during the balance calculations using the least squares method [57] for the high-magnesia basalt from Bulochka satellite cones, indicated that this composition is almost identical to the composition of the real

[2] Due to length restrictions, we omit here the complete data on the calculation of the V_s and V_p/V_s parameters.

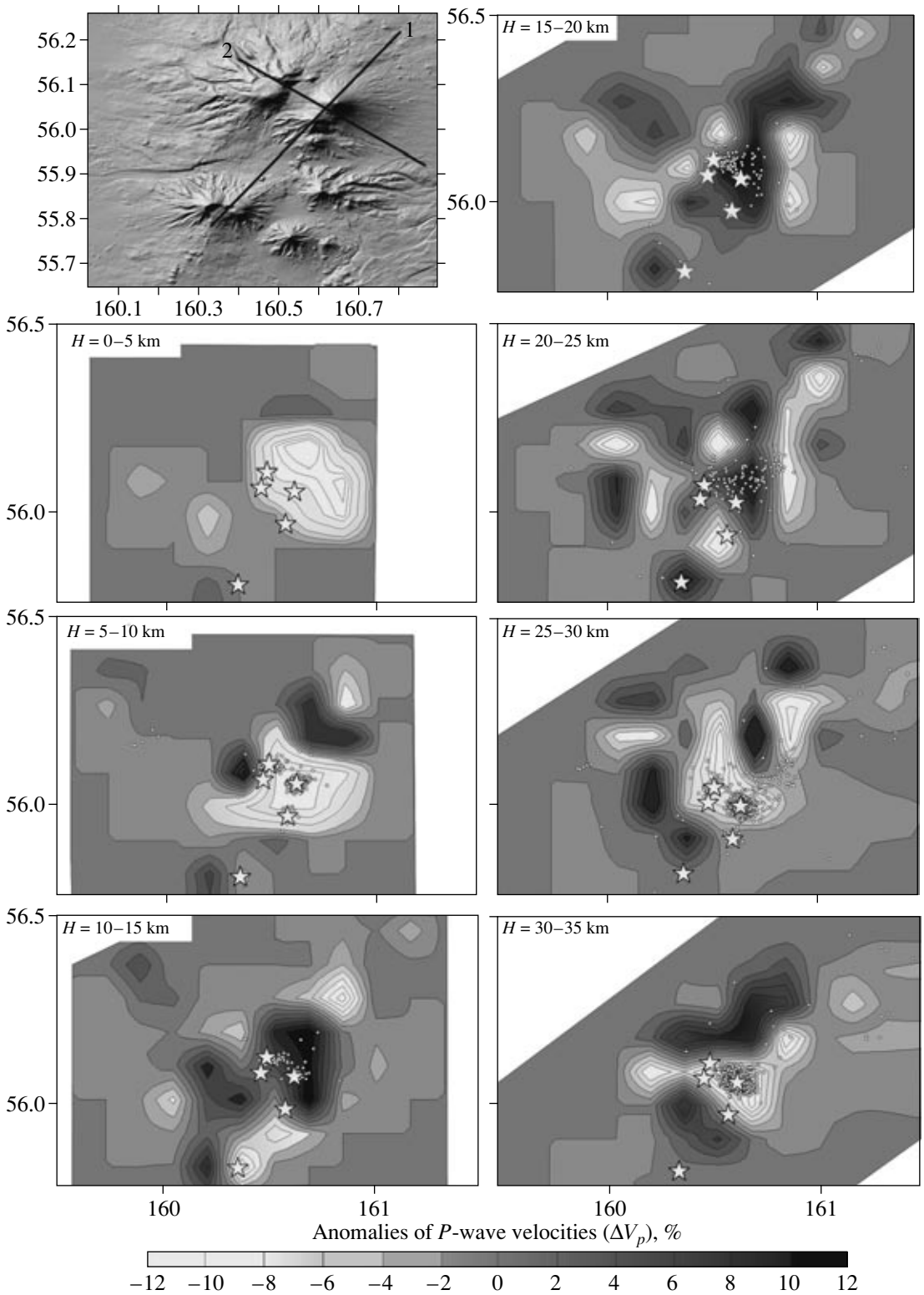

Fig. 2. Horizontal sections of the 3D V_p velocity model of the Earth's crust beneath KVG corresponding to the 0–5, 5–10, 10–15, 15–20, 20–25, 25–30, and 30–35 layers. Asterisks show the location of the volcanoes; circles, that of epicenters of earthquakes with $K_s > 5$. Profiles 1 and 2 correspond to the vertical model sections shown in Fig. 3.

magnesian basalt from Tsirk lateral cone [35]. This directly points to a genetic relation among the entire series of magnesian rocks [35].

The results from studying the major and trace elements of the same samples in the representative set of magnesian and high-alumina basalts obtained by two

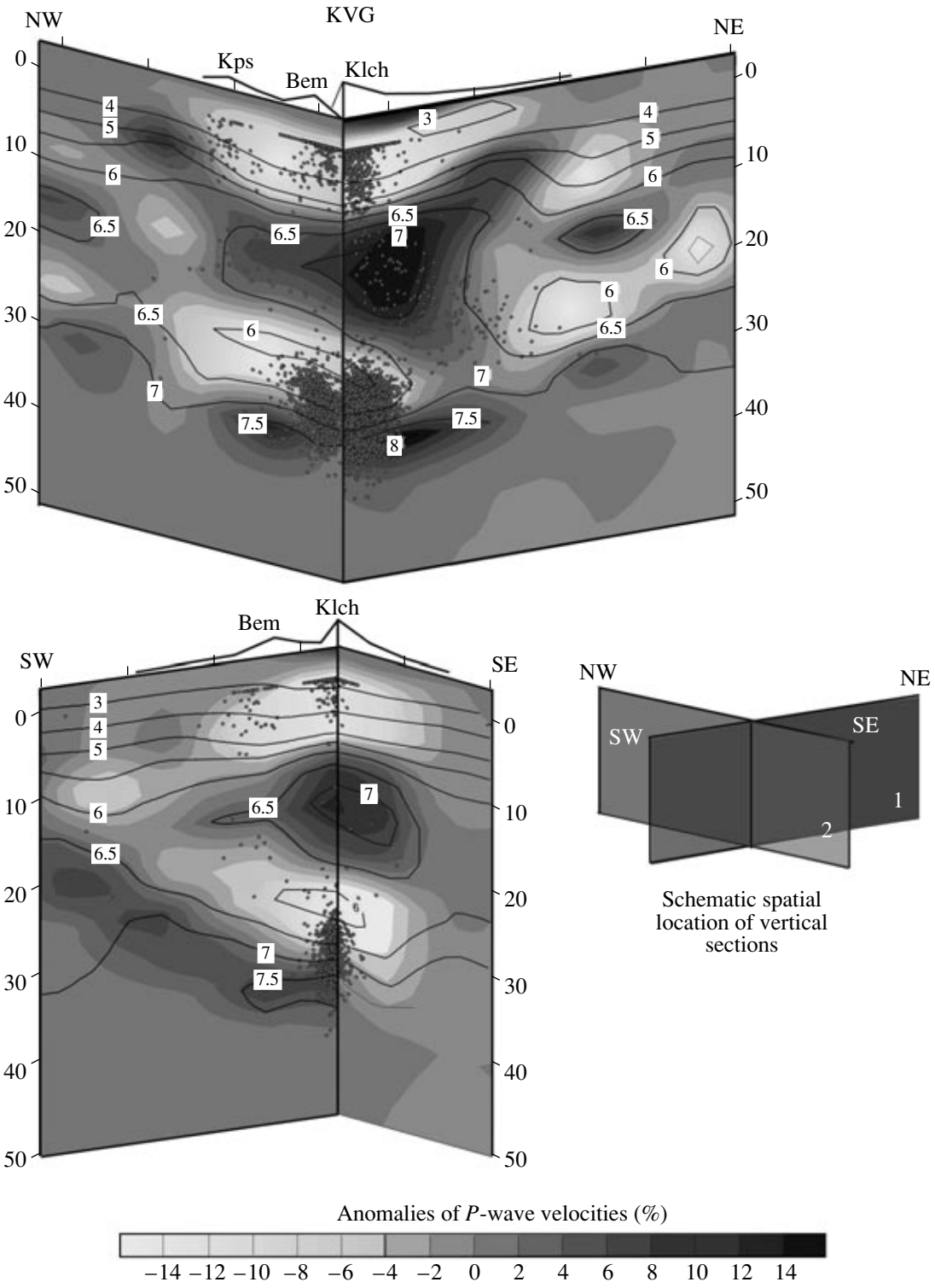

Fig. 3. A 3D image of the velocity model of the Earth's crust beneath KVG. The sections present the contour lines of the absolute values of the V_p velocity (km/s, solid lines) and the projections of earthquake hypocenters onto these sections (circles).

independent methods—inductively coupled plasma mass spectrometry (ICP MS) and instrumental neutron activation analysis (INAA)—show good agreement (Table 1). The very similar (almost coincident) trends of variations in the concentration of trace elements and TiO_2 are clearly defined. The concentrations of U, Sr, Ba, and TiO_2 in lavas decrease and those of Co, Ni, Cr, and Sc increase with increasing Mg content (Fig. 5). In this case a change in the concentrations of iron-group elements can be explained by the fractional crystalli-

Fig. 4. Klyuchevskoy Volcano. Bocche (cones) on the northeastern flank of Klyuchevskoy Volcano are shown in the foreground. Photographed by V.J. Podtobachnyi.

zation or cumulation of olivine and chrome-spinellid in the magma chamber, whereas U, Sr, Ba, and Sc are minor constituents in any early crystalline phase of magnesian basalts. The concentrations of these elements reflect direct geochemical relations between basalts and prove the formation of the latter from a common magma chamber.

This is also confirmed by the results of studying REEs and other incompatible elements in the representative series of magnesian and high-alumina basalts (Fig. 6). These results are presented in the form of a spider diagram where the compositions of basalts are normalized to a primitive mantle composition (according to Hoffman [48]). An analysis of this diagram results in the following conclusions. The studied magnesian basalts are characterized by all the features typical of island-arc magmas: negative anomalies in the concentrations of high field strength elements such as Nb and Ti and distinct positive anomalies in the concentrations of large-ion lithophilous elements such as K, Rb, Ba, Sr, and Hf. A deficit of Rb as compared to Ba is the most characteristic feature of all the studied basalts. The REE spectrum in the studied rocks is characterized by enrichment in light REEs as compared to heavy REEs, which is typical of calc–alkaline magmas. The general conclusion, drawn from our data and publications of other researchers [3, 38, 46, et al.], is that a common mantle source exists for all basalts on the Klyuchevskoy Volcano and that the effect of crustal rocks during their formation is absent.

Mineralogical features of magnesian basalts as indicators of fractional crystallization in intermediate magna chambers. All magnesian basalts from the studied bocche of Klyuchevskoy Volcano are represented by high-magnesia (MgO = 10–12 wt %) clinopyroxene–olivine and magnesian (MgO = 7–10 wt %) clinopyroxene–olivine–plagioclase basalts [35]. In spite of different quantitative relationships between rock-forming minerals and different rock chemistry, the petrographic features of all igneous rocks are similar. The most typical rock feature is a porphyric habit and the presence of large (to 10 mm) glomeroporphyric mono- or polymineral aggregates of olivine and clinopyroxene and isolated phenocrysts of spinellid. In this case the number of olivine phenocrysts in all rock varieties is larger than or equal to that of clinopyroxene phenocrysts. The specific chemistry of olivine and pyroxene, ontogeny, and their quantitative relationships are most pronounced in high-magnesia basalts from Bulochka prehistoric satellite cones.

Olivine is the most widespread mineral of high-magnesia basalts and is encountered among phenocrysts and microlites of the main rock mass. The number of phenocrysts accounts for 12% of the rock volume. Olivine is represented by euhedral crystals with characteristic outlines in the form of hexagons and bevel

Table 1. Concentrations of major elements (mass %) and impurities (ppm) in magnesian and high-alumina Klyuchevskoy basalts

Constituents	1	2	3	4	5	6	7	8	9	10
ISP MS method										
SiO_2	50.8	50.9	52.0	52.3	52.0	51.5	52.97	52.9	53.1	53.7
TiO_2	0.8	0.8	0.8	0.9	0.8	0.8	0.9	0.9	0.9	1.0
Al_2O_3	13.5	14.2	13.4	15.0	14.8	16.3	16.0	17.0	17.0	17.8
Fe_2O_3	9.4	9.4	9.3	9.3	9.0	9.4	9.6	9.3	9.3	9.3
MnO	0.2	0.2	0.2	0.2	0.2	0.2	0.2	0.2	0.2	0.2
MgO	11.6	10.8	10.8	8.7	8.6	8.2	7.1	6.1	6.0	4.7
CaO	10.5	10.4	10.1	9.7	10.2	10.0	9.4	9.0	9.1	8.3
Na_2O	2.3	2.5	2.4	2.9	2.8	3.0	3.1	3.3	3.3	3.6
K_2O	0.5	0.5	0.5	0.9	0.9	0.6	0.9	1.0	1.0	1.1
P_2O_5	0.2	0.2	0.2	0.2	0.2	0.2	0.2	0.2	0.3	0.3
Total	99.7	99.7	99.5	99.8	99.4	100.1	100.0	99.9	100.0	99.8
Ba	185	195	211	285	281	198	302	336	327	402
Be	1.2	1.2	1.2	1.2	1.2	1.2	1.29	1.29	1.2	1.29
Co	41	38	41	34	36	34	32	30	27	27
Cr	928	819	819	493	502	338	217	144	108	40
Cu	70	79	78	84	95	83	88	95	94	112
Ga	16	15	15	19	15	19	14	12	20	15
Ni	197	177	171	116	109	92	67	50	42	29
Rb	12	12	15	16	16	13	18	19	17	22
Sc	37.9	36.7	36.7	34.9	36.2	34	33.5	30.79	31.5	26.1
Sr	234	249	231	311	318	307	329	361	356	356
V	242	248	228	253	237	252	255	259	257	260
Y	17	17	17	19	19	19	22	21	20	22
Zn	70	109	93	75	70	73	79	79	79	88
Zr	59	56	59	71	65	63	78	79	76	95
La	4.54	4.49	4.79	5.89	5.27	4.73	6.15	6.68	6.53	6.99
Ce	17.39	19.77	14.68	24.25	18.39	15.37	18.94	17.43	18.61	22.53
Nd	8.79	9.26	8.91	11.08	10.04	9.68	11.61	12.19	12.06	12.93
Sm	2.73	3.02	2.75	3.40	3.08	2.80	3.30	3.19	3.29	3.53
Eu	0.80	0.85	0.78	0.98	0.92	0.94	0.96	1.01	1.02	1.04
Gd	3.14	3.54	3.21	3.89	3.50	3.02	3.71	3.44	3.67	3.82
Dy	2.83	2.84	2.83	3.19	2.98	3.07	3.35	3.42	3.51	3.60
Er	1.70	1.80	1.74	2.06	1.92	1.80	2.01	1.84	2.01	2.22
Yb	1.37	1.51	1.45	1.66	1.55	1.52	1.73	1.73	1.80	1.87
Lu	0.29	0.28	0.28	0.34	0.30	0.27	0.31	0.27	0.31	0.35
Nd/Sm	3.22	3.07	3.24	3.26	3.26	3.46	3.52	3.82	3.67	3.66
Rb/Sr	0.051	0.048	0.065	0.051	0.050	0.042	0.055	0.053	0.048	0.62

Table 1. (Contd.)

Constituents	1	2	3	4	5	6	7	8	9	10
INAA method										
U	0.26	0.28	0.29	0.39	0.39	0.32	0.43	0.43	0.42	0.51
Nh	0.351	0.378	0.43	0.606	0.639	0.46	0.654	0.689	0.664	0.763
Zr	57	62	53	50	70	67	67	73	89	124
Hf	1.66	1.74	1.81	2.04	2.01	2.02	2.27	2.25	2.35	2.82
Na	0.096	0.096	0.118	0.113	0.117	0.112	0.132	0.136	0.130	0.163
Ba	208	213	235	307	303	221	328	369	354	419
Cs	0.29	0.32	0.39	0.42	0.44	0.32	0.45	0.49	0.39	0.54
Rb	7.9	8.7	9.9	13.3	13.8	10.1	13.8	15.2	14.7	17.2
Sb	0.13	0.15	0.16	0.18	0.23	0.16	0.20	0.23	0.22	0.38
Cr	826	749	742	445	446	320	205	139	103	44
Co	45.6	44	43.4	37.4	35.7	37.1	33.8	31.5	31	28.4
Ni	209	191	187	117	106	97	64	49	39	28
Sc	36.2	34.9	34.5	32.9	33.2	32.4	31.7	29.7	30	25.5
La	4	4.07	4.42	5.72	5.75	4.75	5.96	6.71	6.44	7.34
Ce	8.8	8.7	9.5	11.6	12	10.1	12.4	14.3	13.3	16.1
Sm	2.48	2.52	2.46	2.96	2.89	2.77	3.16	3.38	3.23	3.62
Eu	0.85	0.95	0.88	1	0.98	1	1.08	1.12	1.13	1.21
Tb	0.44	0.444	0.455	0.482	0.46	0.47	0.523	0.543	0.526	0.592
Yb	1.59	1.64	1.56	1.74	1.65	1.75	1.94	1.93	1.97	2.18
As	1.2	1.28		0.88	1.06	1.09	1.22	1.16	1.28	4
Mo	0.54	0.92			1.67	0.83	0.84	0.9	0.88	1.06
Br		0.54	0.7	1.01	1.25			1.16	0.41	0.76
Ag	34		53	45	43			56	42	157
Au	54.89	2.41	238.9	3.23	2.57	26.79	57.95	5.06	1.85	54.85

Note: Magnesian basalts from (**1**) Bulochka, (**2**) Novograblenov, (**3**) Luchitskii, (**4**) Kirgurich, (**5**) Biokos', (**6**) Levashov, (**7**) Tiranus, and (**8**) Nevidimka volcanoes. High-alumina basalts from (**9**) Zavaritskii Volcano and (**10**) the summit eruption of Klyuchevskoy Volcano in 1984.

rhombs. The dimensions of the phenocrysts vary from 0.3 to 2 mm. A purely azonal or slightly zonal magnesian ($Fo_{91.5–88}$) center surrounded by a thin ferrous border is typical of large olivine crystals. Small (5–10 μm) olivine microlites are the lowest in magnesia (Fo_{50}). Studying the statistical distribution of the magnesia content of olivine phenocrysts, based on 280 analyses, makes it possible to conclude that a widely varying composition (from $Fo_{91.5}$ to Fo_{80}) is the most characteristic feature of olivine phenocrysts. In this case, a distinct bimodality is distinguished in the compositions of olivine phenocrysts. The groups of magnesian ($Fo_{91.5–86}$) and more ferrous ($Fo_{85–80}$) olivine are present here. Olivine forms aggregates with clinopyroxene and, sometimes, with chrome-spinellids. Chrome-spinellid and clinopyroxene are often encountered among microinclusions in olivine phenocrysts.

The presence of high-magnesia ($Fo_{91.5}$) olivine, typical of the equilibrium with primary mantle melts, is the most characteristic mineralogical feature of basalts from Bulochka satellite cones. At the same time, the absolute majority of studied olivine phenocrysts [51] cannot be interpreted as products of the mantle xenolith disintegration. In our case this is confirmed by a high CaO content of the studied olivines and by a TiO_2 content of spinels, which are solid-phase inclusions in these olivines [35].

Clinopyroxene. Phenocrysts of clinopyroxene are less widespread than those of olivine in high-magnesia basalts from Bulochka satellite cones by a factor of 2.5. Clinopyroxene phenocrysts account for 5% of the rock volume [35]. An analysis of the statistical distribution of the magnesia content of clinopyroxenes also indicates that this content is widely variable, from Mg#75 to Mg#90 (Fig. 7).[3] It is clear that high-magnesia min-

[3] (Mg# = Mg × 100/(Mg + Fe^{2+}), mol %.

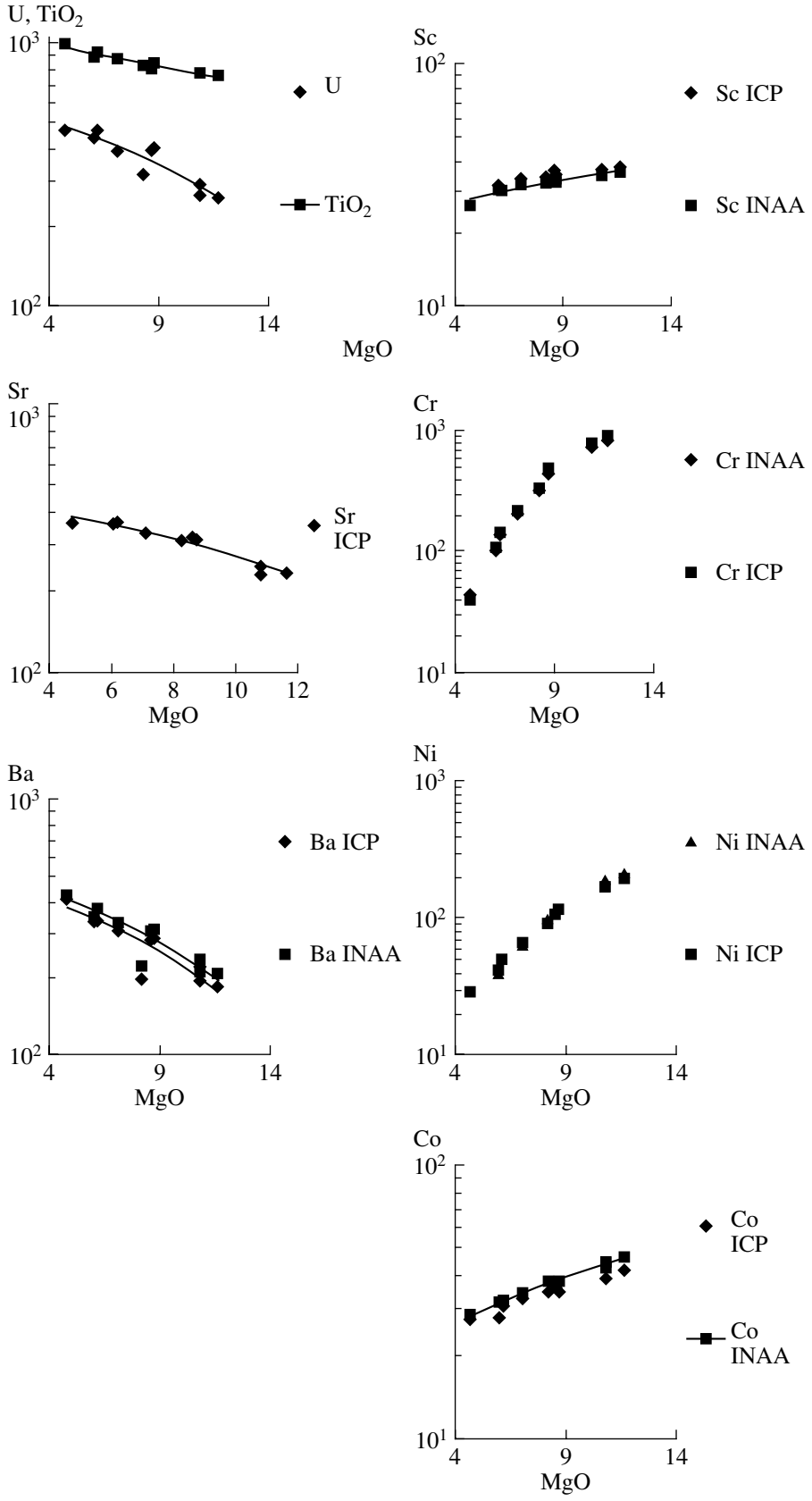

Fig. 5. Dependence of the impurity concentration on the MgO percentage in magnesian and high-alumina basalts from Klyuchevskoy Volcano. (ICP) basalt composition points performed using the ICP MS method and (INAA) basalt composition points performed using the INAA method. The contents of impurities are given in ppm; those of MgO, in wt %.

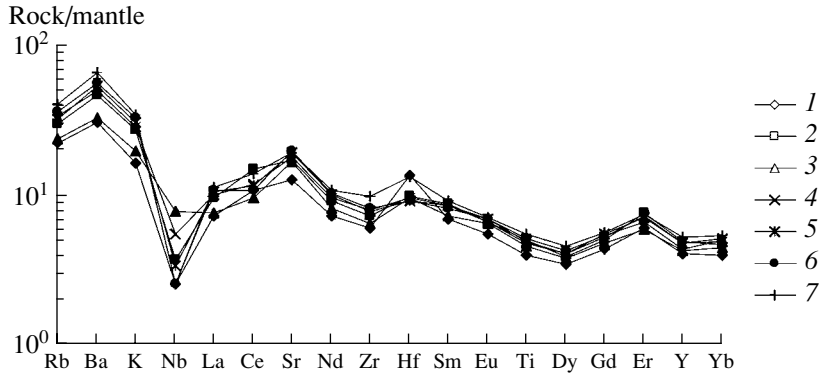

Fig. 6. Spider diagram of magnesian and high-alumina basalts from Klyuchevskoy Volcano. Magnesian basalts from (*1*) Bulochka, (*2*) Biokos', (*3*) Kirgurich, (*4*) Tsirk, (*5*) Tiranus, and (*6*) Nevidimka bocche; (*7*) high-alumina basalt of the 1984 summit eruption. The bocche names are taken from [35]. The composition of a primitive mantle is taken from [48].

eral varieties are almost absent in clinopyroxenes in spite of a widely variable magnesia content. Only 14 of 130 pyroxene crystals taken from a crushed sample have a magnesia content higher than 85. Among phenocrysts, such pyroxene is encountered very rarely and only in aggregates with olivine. At the same time, high-magnesia clinopyroxenes are very often encountered in the form of inclusions in olivines [35]. Clinopyroxene phenocrysts from Bulochka satellite cones are mainly represented by low-magnesia (Mg#85–75) augites, which form aggregates with low-magnesia olivine. Olivine, orthopyroxene, plagioclase, and titaniferous magnetite are encountered in inclusions in low-magnesia clinopyroxenes. The points of the clinopyroxene compositions (see [35]) form regular trends characterized by a sharp decrease in the Cr_2O_3 content and an increase in TiO_2 with decreasing magnesia content of clinopyroxene. The plots of aluminum oxide–magnesia content also show distinct trends toward an increase in the Al_2O_3 content in clinopyroxenes from Bulochka and Bilyukai bocche with decreasing magnesia content [35]. This specific chemistry of low-magnesia clinopyroxenes (augites) is adequately explained by the fractional crystallization of high-magnesia olivines and clinopyroxenes in the early liquidus phases from Bulochka bocche, which could be realized in intermediate magma chambers [35].

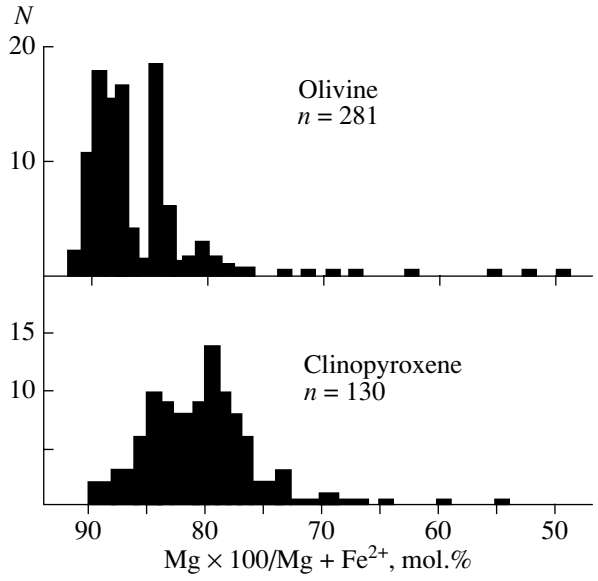

Fig. 7. Distribution of the magnesia content of olivines and clinopyroxenes from Bulochka satellite cones. (N) the number of calculations and (n) the number of analyses.

Chrome-spinellid is identified in the form of inclusions in olivine phenocrysts and is encountered substantially less frequently as independent phenocrysts. The majority of spinels are related to chrompicotite varieties with low TiO_2 [35]. Titaniferous magnetite was encountered in microinclusions of low-magnesia clinopyroxenes from Bulochka satellite cones. Chrompicotite is present in the form of microinclusions only in high-magnesia clinopyroxenes.

All the specific features of the chemistry of clinopyroxenes from Bulochka satellite cones are typical of magnesian basalt phenocrysts from all studied bocche on Klyuchevskoy Volcano. An analysis of the statistical distribution of the clinopyroxene composition of magnesian basalts from the most bocche indicates that these clinopyroxenes are also characterized by a widely variable magnesia content and the absence of bimodality in the composition of clinopyroxenes [35]. Moreover, the above features of the clinopyroxene and olivine chemistry are apparently typical of all calc–alkaline magnesian basalts from this region. In magnesian basalts from Krestovskii Volcano, high-magnesia clinopyroxenes (Mg# higher than 85) constitute negligible part of widespread low-magnesia augites. At the same time, numerous olivine phenocrysts $Fo_{94–90}$, which are only typical of ultrabasic intrusives, are encountered here [35].

The results of studying the statistical distribution of the magnesia content of olivines from basalts in ten bocche, based on 1250 chemical analyses, also indicate

that all magnesian basalts from Klyuchevskoy Volcano are similar in their mineral composition (Fig. 8). High-magnesia ($Fo_{91.5–88}$) olivine was identified in phenocrysts of all rocks. Widely variable compositions (from Fo_{80} to $Fo_{91.5}$) are also typical of phenocrysts in studied olivines. The absence of phenocrysts of low-magnesia olivines in basalts from certain bocche on Klyuchevskoy Volcano (Fig. 8) is caused by the technique of taking of olivine phenocrysts from crushed samples [35]. The highest content of magnesia is observed at the centers of large olivine crystals while the highest iron content is found at thin fringes and the edges of large crystals. Nonequilibrium minerals are evidently present with such a widely variable magnesia content of olivine phenocrysts, even in a single basalt sample. The highest-magnesia ($Fo_{91.5–88}$) olivines in Klyuchevskoy Volcano basalts are generally not typical of basic lavas but are often encountered among olivines in picrites. Such wide ranges of magnesia variations in olivines are typical of picrite basalts from New Georgia, the Solomon Islands [49], picrite sills from New Hebrides [44], picrite magma products of Oshima-Oshima Volcano, Japan [58], etc. Special studies were performed in order to elucidate the olivine composition at the liquidus of magnesian basalts from Klyuchevskoy Volcano.

Calculation of the olivine composition at the liquidus of magnesian basalts. As a result of the detailed studies, it was indicated that, for the large series of natural basalt melts, the composition of olivine at a liquidus slightly depends on crystallization temperature and pressure [39]. Therefore, the present work paid special attention to the degree of iron oxidation in a melt, which substantially affects the composition of crystallized olivine. As was shown in the experimental work [47], chromium spinel is the most sensitive indicator of the degree of iron oxidation (Fe^{2+}/Fe^{3+}) in a basalt melt. The technique and results of the detailed special studies of the dependence of spinel oxidation degree on hosting olivine in the representative series of magnesian basalts from Klyuchevskoy Volcano were published in [35]. The degree of iron oxidation in a basalt melt remained unchanged in the entire spectrum of crystallized olivines ($Fo_{91.5–82}$). This circumstance and ontogeny of phenocrysts of high-magnesia olivines in basalts most likely indicate that olivine phenocrysts ($Fo_{91.5–82}$) crystallized from a sufficiently large magma volume in a closed system, apparently, in the regime of intermediate chambers [35].

The Ford model [39] was used to calculate the composition of olivine at the liquidus. The calculation was based on the fractional model of crystallization. The average bulk-rock chemistry of basalt was taken as the melt composition. The degree of magnesian melt oxidation was taken from [35]. An analysis of the calculation performed for magnesian basalts from ten bocche makes it possible to conclude that $Fo_{91.5}$ olivine cannot be obtained, even when using the highest-magnesia bulk-rock chemistry of basalts from Klyuchevskoy Volcano (Fig. 8). The calculated compositions of olivine at the liquidus in basalt melts from Bulochka ($Fo_{89.7}$) and Bilyukai ($Fo_{84.5}$) bocche are the closest to and most different from this composition, respectively. We should state that real olivine at the liquidus of a basalt melt includes an even lower forsterite constituent, since the bulk-rock chemistry of basalts (during the preparation of the samples for which, nonequilibrium high-magnesia phenocrysts of olivines were also abraded) was used in the calculation. Moreover, we cannot discount the possibility that ascending magma could also be enriched in olivines, due to the processes of accumulation. All high-magnesia intratelluric phenocrysts of olivines are xenocrysts with respect to the transporting melt, since they were formed at a different oxidation potential and from a higher-magnesia initial melt. An analysis of the above data makes it possible to draw a fundamental conclusion on the site of crystallization of the studied olivines and pyroxenes.

1. The systematically low calculated compositions of olivines at the liquidus as compared to their real compositions in basalts, wide ranges of variations in the magnesia content of olivines ($Fo_{91.5–80}$), and the joint occurrence of large azonal high-magnesia ($Fo_{91–88}$) phenocrysts of olivines with low-magnesia ($Fo_{80–81}$) olivines and clinopyroxenes in one sample of magnesian basalts, indicates that phenocrysts of olivines, crystallized from different melts and at different temperatures in intermediate magma chambers of a different level, were mechanically mixed.

2. Cotectic crystallization of Fo_{89} olivine began together with clinopyroxene of close magnesia content [35]. Meanwhile, real phenocrysts of clinopyroxenes with Mg# 85–89 are almost absent in all basalts. These phenocrysts are present in the form of microinclusions in olivines. Real cotectic amounts of phenocrysts are observed only in low-magnesia low-temperature augites with low-magnesia olivines, which probably crystallized under the conditions of low pressures. This indicates that high-magnesia pyroxenes dissolved or precipitated as magma ascended toward the surface, which could be related to a high crystallization initial pressure (the initial pressure for high-magnesia clinopyroxenes) of the magmatic melt in the intermediate chambers. A larger or equal number of olivine phenocrysts as compared to the number of clinopyroxene phenocrysts in all magnesian basalts from Klyuchevskoy bocche indirectly points to such a possibility [35]. Dissolution or precipitation of high-magnesia clinopyroxenes results in enrichment of ascending magma in olivines due to the presence of undissolved high-magnesia olivines ($Fo_{91.5–86}$). The alternative hypothesis, that the considered magma crystallized in the field of olivine, seems to be improbable, due to the presence of phenocrysts of high-magnesia (cotectic for high-magnesia olivines) clinopyroxene in basalts and microinclusions of this clinopyroxene in $Fo_{91.5–86}$ olivines. Thus, we can assume that at least two discrete levels of crystallization depths exist in intermediate magma chambers for low-magnesia clinopyroxenes and oliv-

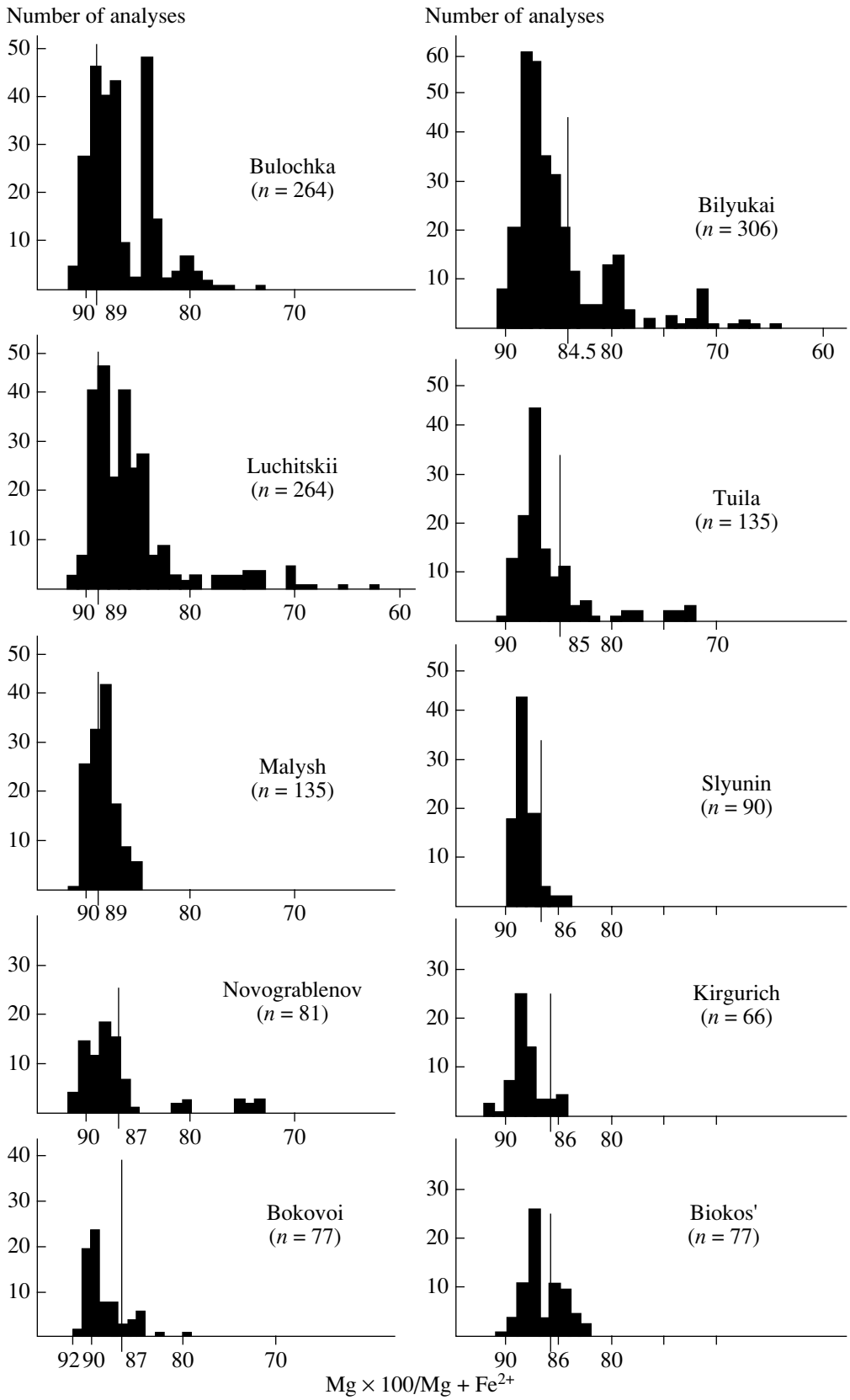

Fig. 8. Distribution of the magnesia content of olivine phenocrysts in magnesian basalts from the Klyuchevskoy bocche. The vertical line corresponds to the calculated olivine composition at the basalt melt liquidus; (*n*) the number of analyses.

ines on the one hand and for high-magnesia olivines and clinopyroxenes on the other hand. Basalts from the Klyuchevskoy bocche evidently represent hybrid rocks including nonequilibrium associations of phenocrysts generated under different conditions. The results from studying the magmatic inclusions in minerals also confirm this statement.

Inclusions in minerals. Inclusions in minerals were studied in magnesian basalts from Bulochka, Slyunin, Tsirk, Bilyukai, Luchitskii, Tuila, Kirgurich, and Biokos' bocche. When we described and classified magmatic inclusions, we used the terminology accepted by I.T. Bakumenko [4]. The following types of primary magmatic inclusions are present in phenocrysts of olivines and clinopyroxenes in the studied rocks: normal melt (vitreous and partially and completely crystallized); crystal; and fluid inclusions. Crystal inclusions are characterized in detail in [35]; therefore, we characterize here fluid and melt inclusions.

Fluid inclusions. Fluid inclusions in olivines of magnesian basalts from Klyuchevskoy Volcano were studied in a cryocamera designed by Simonov (IG i G SO RAN) in the temperature range from –90 to +40°C. A standard inclusion of CO_2 was used in the experiments. Fluid inclusions in high-magnesia olivines are represented mainly by dense carbon dioxide. The characteristic thermometric parameters of fluid inclusions (triple point temperature, –57.3°C, and temperature of homogenization into a liquid phase, 28°C) indicate that the composition of a magmatic fluid is substantially carbon-dioxide, which is confirmed by the data of Raman spectroscopy (Fig. 9) obtained at the Center of Petrography and Mineralogy in Nancy (France) using the Dubessy technique [56]. According to these data, the CO_2 in a fluid inclusion in olivine from magnesian basalts of Bulochka satellite cones was more than 99 mol % of that found in the fluid phase (ignoring H_2O). The total percentage of CO, N_2, CH_4, H_2S, and SO_2 in this inclusion was not more than 0.5 mol %. The maximal density measured in several fluid inclusions in olivines is 0.85 g cm^{-3} (homogenization of gaseous CO_2 into a liquid phase occurred at a temperature of 28°C). The crystallization pressure of magnesian basalts was calculated based on these data, the maximal measured temperature of a CO_2 fluid (0.85 g cm^{-3}), and the experimental dependence of pure CO_2 density on pressure and temperature [7], taking into account a temperature of 1280°C (see below). The minimal crystallization pressure, calculated based on the density of fluid inclusions in olivines, is 5–6 kbar (15–18 km). We should emphasize that this is the minimal crystallization pressure of olivines ($Fo_{88–87}$) since relatively large fluid inclusions are often subjected to decrepitation and, consequently show decreased values of density and pressure. Indeed, numerous small and higher-density inclusions, which should be considered independently, are encountered in olivine.

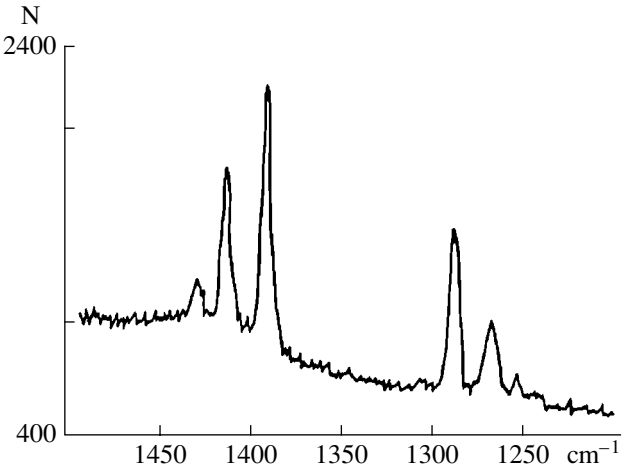

Fig. 9. Raman scattering spectra of CO_2 in an olivine fluid inclusion; (N) the spectrum intensity.

All studied fluid inclusions in low-magnesia clinopyroxenes (augites) have a low density without a visible phase boundary at temperatures of 18–20°C, which indicates that these inclusions crystallized at low pressures (within 1–2 kilobars) at depths of approximately 1–6 km.

Melt inclusions. Normal melt inclusions are represented by vitreous and partially and completely crystallized varieties. In olivine and clinopyroxene, these inclusions are often confined to the zones of growth, especially at outer borders of minerals, but are also encountered as isolated inclusions occasionally located in a host matrix.

In clinopyroxene, inclusions have different shapes: from irregular to isometric. Inclusion dimensions vary from 2 to 30 μm. The inclusion phase composition is as follows: glass + gas, glass + gas + ore mineral, and glass + gas + ore mineral + plagioclase.

In olivine, inclusions are as a rule rounded, sometimes, semifaceted. The size of inclusions in olivines, as in clinopyroxene, is widely variable: from 2 to 50 μm. In olivine large isolated vitreous inclusions are encountered more frequently. The phase composition of inclusions is more variegated: glass + gas, glass + clinopyroxene + gas, glass + clinopyroxene + chrome-spinellid + gas, and glass + chrome-spinellid + gas.

Melt microinclusions have primarily been studied by optical thermometry [25, 28]. The behavior of olivine during heating substantially differs from that of clinopyroxene. The temperature of low-magnesia clinopyroxene (augite) homogenization increases with increasing experimental time. This process, related to the process of H_2O decomposition in an inclusion, was described in detail by one of the authors of the present work during homogenization of clinopyroxene in Hawaiitian lavas from the Etna Volcano, Sicily [26]. The maximal temperature of homogenization of melt

inclusions augites (Mg#85) from Klyuchevskoy basalts was 1200°C, and the minimal homogenization temperature for Mg#75 augites was 1080°C.

We failed to reach a complete homogenization of the melt inclusions in olivine. The volume of a gas bubble stops decreasing at a temperature corresponding to the melting of the daughter crystalline phases of clinopyroxenes (1190–1230°C) and remains constant until complete decrepitation of inclusion at a temperature of 1450–1500°C (Fig. 10). When decrepitation does not take place and the heating time is more than 40 min, a gas bubble at a temperature of 1500°C can run through a vacuole wall and appear in an olivine body. In studied olivines from magnesian basalts, it is only possible to operate with large (20–30 μm) inclusions. Operation with smaller inclusions results in autoxidation, even with an insignificant heating time (less than 5 min). A similar process was described in more detail by one of the authors [27]. The method of fusion to the last crystal described in [13] was used to study melt inclusions in olivines. An inclusion was brought to the melting of the last crystal of a daughter mineral, clinopyroxene, and was guenched after the minimal (less than 5 min) heating time (Fig. 10). The calculated olivine crystallization temperatures were 1330–1370°C [36].

Parent melt of magnesian basalts from Klyuchevskoy Volcano. The composition of guenched, partially homogenized, melt inclusions at the temperature of melting of the last daughter crystal are presented in [36]. The composition of the parent melt was determined by numerical simulation of the inverse fractional crystallization in the olivine field, from the state corresponding to guenched melt inclusions, to the equilibrium with the highest actually identified MgO olivine content ($Fo_{91.2}$) [36]. The composition corresponds to picrite with an ultimate saturation of SiO_2. We should note that increased SiO_2 contents of Klyuchevskoy basalts are one of the most pronounced features (petrochemical face), which make it possible to distinguish these basalts from other magnesian basalts, e.g., from basalts in the Northern satellite cones of Great Tolbachik Fissure Eruption [6]. Academician A.N. Zavaritskii [14] pointed out this feature of the chemistry of the Klyuchevskoy basalts. The degree of iron oxidation in a melt, necessary for calculation models, was determined based on the spinel–melt equilibrium [47]. The obtained estimates of oxygen fugacity are close to that for the quartz–fayalite–magnetite buffer [36].

The percentages of Ti, Cr, Zr, Sr, Hf, Y, Nb, Ba, REEs, and H_2O) impurities in guenched glass of 13 homogenized melt inclusions in olivine phenocrysts in magnesian basalts from Klyuchevskoy bocche were obtained using the method of secondary-ion mass spectrometry (Table 2). All melt compositions show evident indications of island-arc magmas (Fig. 11), namely: high (excess on a spider-diagram) concentration of large-ion lithophilous elements (Ba, K, Sr) and anomalously low concentration of high-charge cations (Ti, Zr, Nb). High H_2O content is the most pronounced feature of parental melts of Klyuchevskoy Volcano (Table 2). The ratio of H_2O to Al_2O_3 is almost independent of the fractionation of the early liquidus phases (olivine, clinopyroxene, and chrome-spinellid) and, consequently, can represent these phases in parent melts [36, 53]. However, the measured ratios in melt inclusions are characterized by considerable variations independent of the composition of the hosting olivine (Table 2). This can be related to a partial loss of water from melt inclusions under natural conditions and during the experiment [28, 43]. Therefore, the largest values from the interval $H_2O/Al_2O_3 = 0.17–0.21$, corresponding to 2.2–2.9 mass % of H_2O in a parent melt [36], are the most real. The obtained H_2O contents of primitive island-arc magmas are higher than the earlier estimates [55] by a factor of 2–3 and are the first reliable determinations of the initial H_2O content of parent magmas typical of the island-arc series [36]. The most similar H_2O contents of initial magmas published in [52] corresponded to substantially fractionated island-arc andesites, rather than to primitive magmas, as were found in our case.

The geochemistry of the magnesian basalts gives additional information about the parent melts and their sources. As was indicated previously, the concentrations of major elements and impurities indicate that magnesian basalts belong to typical island-arc rocks (Table 1). These basalts are enriched in large-ion lithophilous elements and are depleted in high field strength elements, especially Ti and Nb. Such a typical geochemistry of island-arc magmas is traditionally described as the mixing of two independent components characterizing the sources of these magmas: a strongly depleted "dry" material—the mantle wedge beneath an island arc located above a subduction zone—and a component that is either a melt of island-arc magma or a product of subduction plate degassing. This plate may introduce the major portion of water and the elements with large radius ions into magma. This is also confirmed by the most recent data from Pb isotopy [38]. The geochemistry of the studied lavas generally does not contradict such a model. An evident disproportion in the relationship between Rb and Ba (i.e., a deficit of Rb with respect to Ba), shown on the spider-diagram, makes it possible to assume that a phase including Rb (apparently, phlogopite) should be present in the low temperature mantle or slab. According to Hoffman [48], the amount of both components (Rb and Ba) in oceanic sediments is approximately the same as in the primitive mantle. Since phlogopite is unstable under high pressures, the assumption that this mineral is present in the residue makes it possible to estimate the ultimate depth from which the subduction component of the source could come.

The conditions of generation of the primary magmas were assessed based on the magma composition and the assumption that these magmas are in equilib-

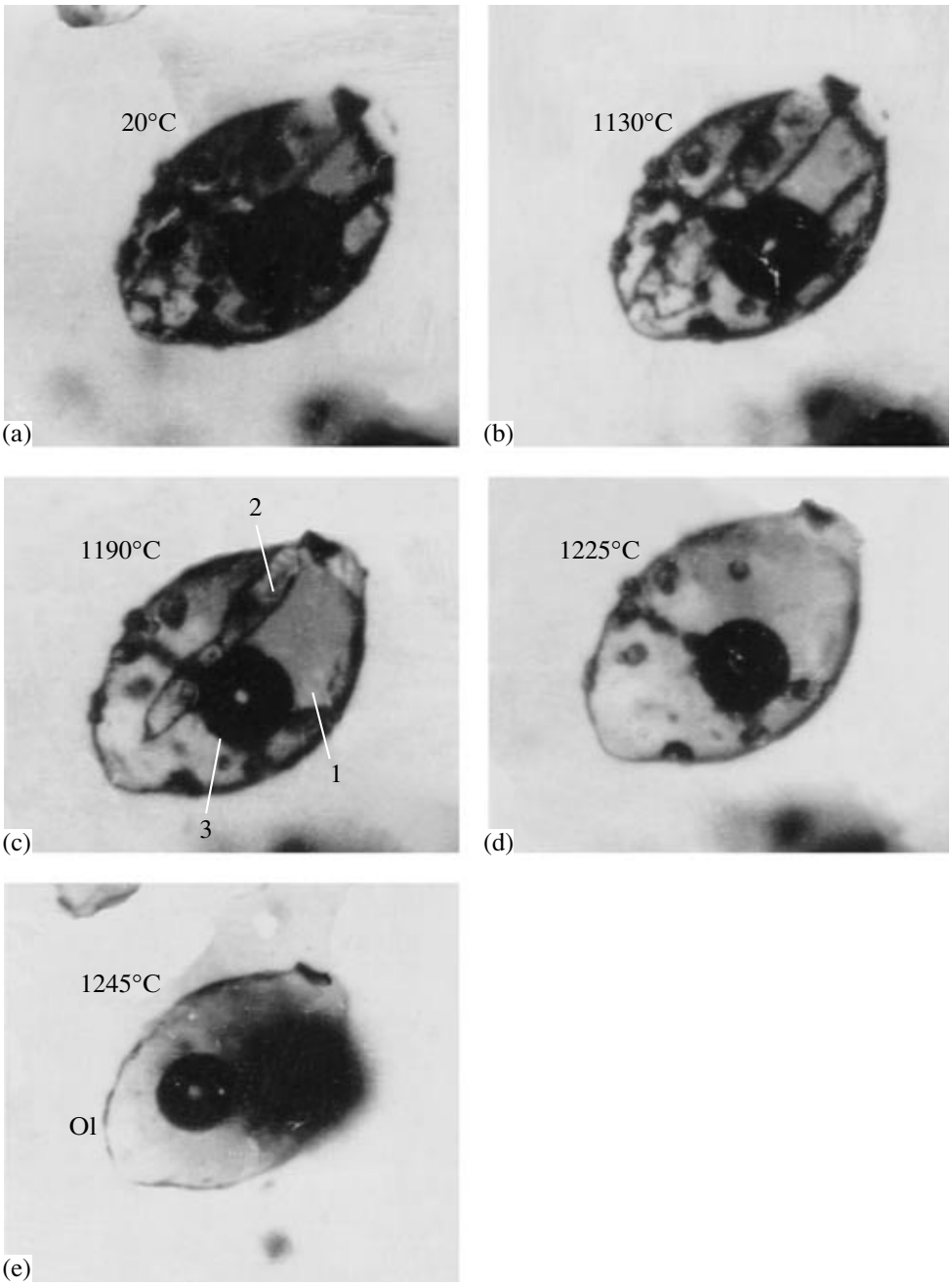

Fig. 10. Microphotographs of the melting of a partially crystallized melt inclusion in hosting olivine of magnesian basalt from Bulochka satellite cones. (a) Melt inclusion before the experiment at an ambient temperature, (b)–(d) intermediate stages of melt inclusion melting, (e) partially homogenized melt inclusion at the end of the experiment. Phase indices: (Ol) hosting olivine (Fo_{88}), (1) melt, (2) clinopyroxene daughter crystal, and (3) shrinkage gas bubble. Numerals indicate the microinclusion melting temperature.

rium with the mantle material of the lherzolite–harzburgite series [36]. Such an assessment was performed based on the standard diagram Ol–Pl–Q–Di with isobars determined from the experimental data in the presence of H_2O [41, 54]. The obtained data make it possible to conclude that the melt separated from the mantle material at pressures of 15–20 kbar (with an estimation accuracy of 3 kbar). This pressure estimate corresponds to a magma melting depth of 40–60 km, in good agreement with magma chamber depth estimates obtained from tomography data and [10, 32, 33]. The temperature of the parent melt separation, 1280–1320°C (see [36]), was estimated using the algorithm presented in [53], based on the melt composition (MgO = 13.5 mass %), water content of this melt (2.9 mass %), and separation pressure (15–18 kbar).

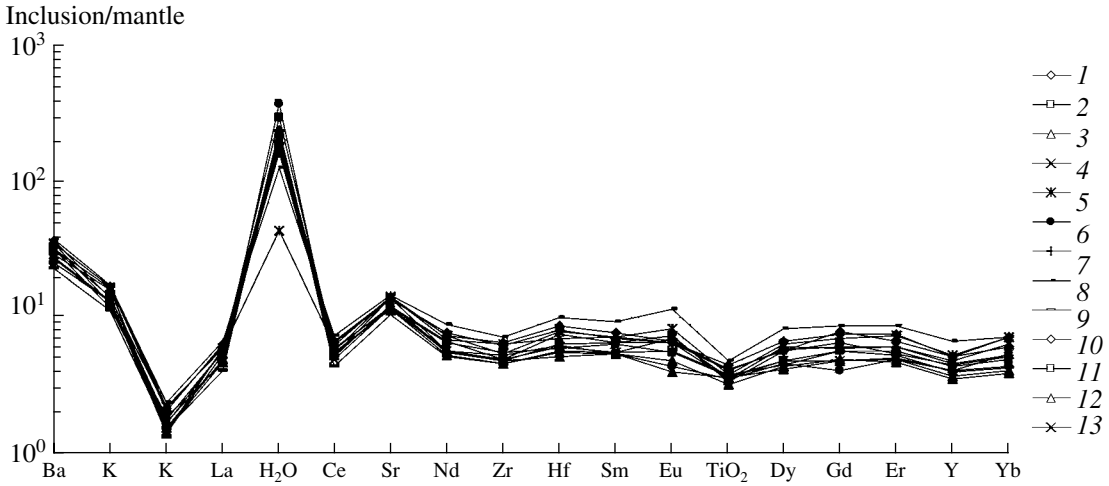

Fig. 11. Spider diagram of partially homogenized melt inclusions in olivines of magnesian basalts from Klyuchevskoy Volcano. The compositions of inclusions in olivines of basalts from (*1*) and (*2*) Bulochka, (*3*) Luchitskii, (*4*)–(*8*) Tuila, (*9*) and (*10*) Kirgurich, and (*11*)–(*13*) Biokos' bocche. The satellite cones names are taken from [35].

RELATIONSHIP BETWEEN PETROLOGICAL ESTIMATES AND RESULTS OF SEISMIC TOMOGRAPHY

The above assessments of the conditions of generation of high-magnesia melts from the Klyuchevskoy Volcano make it possible to generally represent the 3D model of formation of magnesian basalts based on the petrological and geophysical data.

The first level corresponds to the depth of melt separation from the melt residue (40–60 km) at a temperature of 1280–1320°C. Here, picritic melts can form and move along the system of fissures toward the site of fractionation in the intermediate magma chambers. This conclusion is in adequate agreement with the calculations of the asthenospheric depth and comparison of the theoretical and experimental velocity (V_p) models [9, 19]. This conclusion also does not contradict other previous studies [10, 32]. Many long-period earthquakes are generated at depths of 20–40 km beneath Klyuchevskoy Volcano. Such events at the crust–mantle boundary are also registered at other volcanoes located worldwide. The origin of these events is related to the intrusion of a magma melt from a mantle diapir into the Earth's crust [12, 37, 45, 59]. We should note that the existence of the magma source prior to the separation of this source from the mantle residue, at depths below those indicated above, suggests systematic repeated equilibrium between the melt and the mantle residue; therefore, the composition of this melt is unknown.

The second level, through which magnesian basalts are formed and which is registered based on fluid microinclusions in olivines, corresponds to a minimal pressure of 5–6 kbar and a depth of more than 18–20 km at a maximal temperature of 1280°C (taking the 2.9% of water in the melt into account). Stable intermediate chambers, where picritic magmas crystallized and fractionated, are apparently generated here. Taking the errors of the method into account, this depth is in good agreement with the 25–30 km depths, where the method of seismic tomography makes it possible to reliably register low-velocity V_p and V_s anomalies and increased values of the V_p/V_s parameter, which are most likely related to a magma chamber. The results of other geophysical methods and theoretical calculations also indicate that a dynamically related system of magma chambers could exist in this layer [6, 32].

A high-velocity discontinuity was reliably distinguished at a depth of 10–20 km beneath the Klyuchevskoy Volcano in the middle part of the Earth's crust (anomalies of the V_p and V_s velocities reach 10% in this region). This anomaly is most probably related to an ancient crystallized intermediate chamber, which supplied the Ushkovskii and Krestovskii volcanoes 40–50 ka ago. The presence of a high-velocity discontinuity is evidently an insurmountable obstacle for a direct magma duct from the mantle to the Klyuchevskoy crater. We should note that the methods of seismic tomography also made it possible to distinguish high-velocity zones, which are interpreted as large intrusions of crystallized ultrabasic–basic magmas, in the Earth's crust beneath other volcanoes located worldwide [37, 45].

In addition to calc–alkaline magnesian basalts, calc–alkaline high-alumina basalts and andesites magnesian melts also erupt within the Klyuchevskoy volcanic group. According to modern petrological studies their occurrence is also related to a mantle supply and the further fractionation of magnesian melts [1, 16]. The genesis and conditions of generation of these igneous rocks are outside the limits of this publication. However, these eruptions stimulate researchers to study the spatial location of intermediate magma chambers, where magnesian and high-alu-

Table 2. The composition of olivine and melt inclusions in magnesian basalts from Klyuchevskoy Volcano

Constituents	1	2	3	4	5	6	7	8	9	10	11	12	13
Hosting olivine													
SiO_2	40.78	41.73	40.64	40.73	41.21	40.36	40.30	41.43	40.94	40.44	41.10	41.15	41.16
MgO	47.94	48.00	46.86	47.78	48.29	47.19	46.70	48.70	47.10	46.76	47.20	48.20	48.13
FeO	10.68	9.99	11.72	10.57	10.72	11.43	11.49	9.91	11.92	12.10	12.66	10.67	9.64
MnO	0.01	0.01	0.02	0.03	0.02	0.00	0.02	0.01	0.03	0.02	0.04	0.01	0.01
CaO	0.18	0.24	0.15	0.26	0.25	0.19	0.14	0.24	0.20	0.21	0.18	0.25	0.19
NiO	0.11	0.20	0.20	0.15	0.19	0.14	0.14	0.24	0.20	0.12	0.17	0.16	0.14
Total	99.70	100.17	99.59	99.52	100.68	99.31	98.79	100.53	100.39	99.65	101.35	100.44	99.27
Fo	89	90	88	89	89	88	88	90	88	87	87	89	90
Melt inclusions													
H_2O	1.78	2.46	1.47	2.00	1.69	0.37	3.16	1.35	1.04	1.96	1.63	1.53	1.92
Ti	5233	4674	5405	4210	4342	4453	4155	4684	5999	4369	5248	4542	4098
Cr	464	338	188	459	363	227	203	335	335	291	252	340	328
Sr	247	215	262	215	217	260	224	223	266	194	256	256	214
Y	20.40	17.60	19.30	14.60	16.40	20.90	16.10	18.00	26.30	16.00	20.60	17.80	14.10
Zr	60.70	54.30	62.80	47.40	48.60	53.20	51.40	47.70	71.10	45.30	64.10	47.60	44.90
Nb	1.35	1.12	1.37	0.96	0.92	0.90	1.07	1.03	1.47	0.95	1.27	1.17	0.88
Ba	221	194	211	177	165	192	152	209	228	140	211	192	172
La	3.78	3.53	3.69	3.04	2.94	3.72	2.96	3.49	4.13	2.55	3.95	2.87	3.33
Ce	10.61	9.61	9.19	8.61	8.05	10.06	8.28	9.33	11.97	7.15	10.84	8.63	8.99
Nd	9.20	7.90	8.12	6.66	6.76	8.78	6.81	8.06	10.74	6.21	8.92	6.86	6.34
Sm	2.73	2.49	2.79	2.09	2.18	2.80	2.12	2.56	3.67	2.15	2.99	2.57	2.13
Eu	2.51	2.17	2.45	1.82	2.19	2.56	1.71	2.43	3.30	1.82	2.46	2.42	1.92
Gd	6.07	4.88	5.17	4.28	4.16	5.56	3.63	5.25	6.72	4.36	6.19	5.26	4.29
Dy	4.27	3.08	3.90	2.71	3.09	4.07	2.95	3.74	5.27	2.85	3.63	3.66	2.82
Er	3.14	2.41	2.56	2.08	2.12	3.10	2.06	2.56	3.65	2.22	2.81	2.29	1.99
Yb	2.98	2.07	2.66	1.68	2.24	3.01	1.81	2.21	2.98	1.79	2.54	2.14	1.62
Hf	1.67	1.24	1.45	1.09	1.27	1.65	1.29	1.57	2.11	1.19	1.79	1.32	1.15

Note: (**1**)–(**12**) Compositions of melt inclusions is olivines of magnesian basalts from Klyuchevskoy bocche: (**1**) and (**2**) Bulochka, (**3**) Luchitskii, (**4**)–(**7**) Kirgurich, (**8**)–(**10**) Tuila, (**11**)–(**13**) Biokos'. The compositions of oxides and impurities are given in mass % and ppm, respectively. The names of the cones are taken from [35].

mina magmas could fractionate, leading to the occurrence of andesite melts [1, 2, 16, 20, et al.]. These chambers could be located on both sides of the crystallized intrusion at depths of 10–20 km, where increased values of the V_p/V_s parameter were obtained from the data of seismic tomography.

The third level, where magnesian magmas can crystallize and fractionate, corresponds to low pressures, apparently, within several kilobars. This level can only be assessed indirectly based on the absence of a high-density fluid in the augite of magnesian basalts. Low crystallization pressures of augites are also confirmed by the ability of the augite-hosted meld inclusion to homogenize. Associations of high-pressure phenocrysts mix with low-pressure crystallization products in these shallow chambers. Boris Ivanovich Piip [22] substantiated the existence of intermediate chambers at the same depth (5–7 km) beneath the northeastern flank of Klyuchevskoy Volcano based on xenoliths of Tertiary rocks from bocche. According to [5, 23], velocity anomalies are confined to the same depth. The calculations in [16] indicate that shallow-depth crystallization of clinopyroxenes in high-alumina magmas occurs beneath the northeastern flank of Klyuchevskoy Volcano. All these conclusions do not contradict the above seismotomographic model. For example, increased values of the V_p/V_s parameter are confined to the Earth's crust depths of 5–10 km. Anomalies of this parameters are most likely related to the presence of shallow-depth magma chambers. Differentiated magnesian and high-alumina magmas, which have provoked lateral eruptions of magnesian and high-alumina basalts on the northeastern flank of the Klyuchevskoy Volcano, could have come from this region during the entire Holocene.

ACKNOWLEDGMENTS

We are grateful to Academician S.A. Fedotov, Professor E. Kissling (University of Zurich), S.L. Senyukov, and I.A. Sanina for constructive discussion of the materials in this paper; to V.M. Chubarov and T.M. Filosofova for help in microprobe analyses; to Doctor J. Dubessy for help in determining the composition of a fluid inclusion using Raman scattering spectroscopy, to Doctor J.-L. Joron and analysts from CRPG (Nancy, France) for rock analysis, to S.K. Simakin for an analysis of H_2O and impurities in melt inclusions, and to N.P. Egorova and L.G. Osipenko for the help in figure preparation.

This work was supported by Program 16 of the fundamental studies of the Presidium of the Russian Academy of Sciences (project 2.7), the Russian Foundation for Basic Research (project no. 06-05-65234), and the President of the Leading Scientific School of the RF (grant NSh-4264.2006.5).

REFERENCES

1. Al'meev, R.R., Geochemistry of Bezymyannyi Volcano Magmatism: Mantle Source Indications and Conditions of Initial Magma Fractionation, *Cand. Sc. (Geol.–Min.) Dissertation*, Moscow: 2006.
2. Anosov, G.I., Bikenina, S.K., Popov, A.A., et al., *Glubinnoe seismicheskoe zondirovanie Kamchatki* (Deep Seismic Sounding of Kamchatka), Moscow: Nauka, 1978.
3. Ariskin, A.A., Barmina, G.S., Ozerov, A.Yu., and Nil'sen, R.L., Genesis of Hich-Alumina Basalts from Klyuchevskoy Volcano, *Petrologiya*, 1995, vol. 3, no. 5, pp. 496–521.
4. Bakumenko, I.T., *Ispol'zovanie metodov termobarogeokhimii pri poiskakh i izuchenii rudnykh mestorozhdenii* (Application of the Methods of Thermobarogeochemistry in Exploration and Study of Ore Deposits), Moscow: Nedra, 1982.
5. Balesta, S.T., Gontovaya, L.I., Kargopol'tsev, V.A., et al., Results of Geochemical Studies of the Eart's Crust in the Region of Klyuchevskoy Volcano, *Vulkanol. Seismol.*, 1991, no. 3, pp. 3–18.
6. *Bol'shoe treshchinnoe Tolbachinskoe izverzhenie, Kamchatka, 1975–1976 gg* (Great Tolbachik Fissure Eruption, Kamchatka, 1975–1976), Moscow: Nauka, 1984, p. 637.
7. Vukalovich, M.P. and Altunin, V.V., *Teplofizicheskie svoistva dvuokisi ugleroda* (Carbon Dioxide Thermophysical Properties), Moscow: Atomizdat, 1965.
8. Gontovaya, L.I., Stepanova, M.A., Khrenov, A.P., and Senyukov, S.L., Depth Model of the Lithosphere in the Region of the Klyuchevskoy Group of Volcanoes (Kamchatka), *Vulkanol. Seismol.*, 2004, no. 3, pp. 3–11.
9. Gontovaya, D.I. and Gordienko, V.V., Deep Processes and Geological Models of the Mantle within Eastern Kamchatka and the Kronotskii Bay, in *Geologiya i poleznye iskopaemye Mirovogo okeana* (Geology and Minerals of the World Ocean), Kiev: NANU, 2006, issue 2, pp. 107–121.
10. Gorshkov, G.S., On a Depth of the Magma Chamber of Klyuchevskoy Volcano, *Dokl. Akad. Nauk SSSR*, 1956, vol. 106, no. 4, pp. 703–705.
11. Gorel'chik, V.I., To the History of Development of Seismological Studies on Kamchatka Volcanoes, in *Geodinamika i vulkanizm Kurilo-Kamchatskoi ostrovoduzhnoi sistemy* (Geodynamics and Volcanism of the Kurils–Kamchatka Island-Arc System), Petropavlovsk-Kamchatskii, 2001, pp. 141–151.
12. Gorel'chik, V.I. and Storcheus, A.V., Deep Long-Period Earthquakes beneath Klyuchevskoy Volcano, Kamchatka, in *Geodinamika i vulkanizm Kurilo-Kamchatskoi ostrovoduzhnoi sistemy* (Geodynamics and Volcanism of the Kurils–Kamchatka Island-Arc System), Petropavlovsk-Kamchatskii, 2001, pp. 173–189.
13. Gurenko, A.A., Sobolev, A.V., Polyakov, A.I., and Kononkova, N.N., Primary Melt of Rift Tholeiites in Iceland: Composition and Crystallization Conditions, *Dokl. Akad. Nauk SSSR*, 1988, vol. 301, no. 1, pp. 179–184.
14. Zavaritskii, A.N., *Severnaya gruppa vulkanov Kamchatki* (Northern Group of Kamchatka Volcanoes), Moscow: Akad. Nauk SSSR, 1935.
15. Zubin, M.I., Kozyrev, A.I., and Luchitskii, A.I., Gravitational Model of the Structure of Klyuchevskoy Volcano

(Kamchatka), *Vulkanol. Seismol.*, 1990, no. 5, pp. 76–93.

16. Mironov, N.L., Portnyagin, M.V., Plechov, P.Yu., and Khubunaya, S.A., Final Stages of Evolution in Klyuchevskoy Volcano, Kamchatka: Evidence from Melt Inclusions in Minerals of High-Alumina Basalts, *Petrologiya*, 2001, vol. 9, no. 1, pp. 51–69 [*Petrology* (Engl. Transl.), 2001, vol. 9, no. 1, pp. 46–62].
17. Melekestsev, I.V., Braitseva, O.A., Erlikh, E.N., et al., *Kamchatka, Kuril'skie i Komandorskie ostrova* (Kamchatka, Kurils, and Commander Islands), Moscow: Nauka, 1974.
18. Moroz, Yu.F. and Nurmukhamedov, A.G., Depth Geoelectric Model for the Region of Conjugation of the Kurils–Kamchatka and Aleutian Islands Arcs, *Fiz. Zemli*, 2004, no. 6, pp. 54–67.
19. Nizkous, I.V., Tomographic Reconstruction of the Kamchatka Region with a High Spatial Resolution, *Cand. Sc. (Geol.–Min.) Dissertation*, Moscow, 2005.
20. Ozerov, A.Yu., Evolution of Basite Melts in the Klyuchevskoy Volcano Feeder System, in *Petrologiya i metallogeniya bazit-giperbazitovykh kompleksov Kamchatki* (Petrology and Metallogeny of the Basite–Ultrabasite Kamchatka Complexes), Petropavlovsk-Kamchatskii, 2000, pp. 58–60.
21. *Ocherki tektonicheskogo razvitiya Kamchatki* (Sketches of the Kamchatka Tectonic Development), Moscow: Nauka, 1987.
22. Piip, B.I., *Klyuchevskaya sopka i ee izverzheniya v 1944–1945 gg. i v proshlom* (Klyuchevskoy Volcano and Its Eruptions in 1944–1945 and in the Past), Moscow: Akad. Nauk SSSR, 1956.
23. Piip, V.B., Efimova, E.A., and Gontovaya, L.I., Interpretation of Time–Distance Plots of Seismic Waves along the CMRW profile in the Region of Klyuchevskoy Volcano, *Vulkanol. Seismol.*, 1991, no. 5, pp. 83–91.
24. Smirnov, V.S. and Bolabko, G.T., Resisticity Anomalies in the Region of the Klyuchevskoy Volcani Group, in *Glubinnoe stroenie, seismichnost' i sovremennaya deyatel'nost' Klyuchevskoi gruppy vulkanov* (Depth Structure, Seismicity, and Recent Activity of the Klyuchevskoy Volcanic Group), Vladivostok, 1976, pp. 7–17.
25. Sobolev, A.V., Melt Inclcusions in Minerals as a Source of Principal Petrological Information, *Petrologiya*, 1996, vol. 4, no. 3, pp. 228–239 [*Petrology* (Engl. Transl.), 1996, vol. 4, no. 3, pp. 209–220].
26. Sobolev, A.V., Kamenetskii, V.S., Metrik, N., et al., Regime of Volatiles and Conditions of Crystallization of Hawaiitian Lavas from Etna Volcano, Sicily, *Geokhimiya*, 1990, no. 9, pp. 1277–1289.
27. Sobolev, A.V. and Nikogosyan, I.K., Petrology of Long-Lived Mantle Jet Magmatism; Hawaiian (the Pacific) and Reunion (the Indian) Islands, *Petrologiya*, 1994, vol. 2, no. 3, pp. 131–168.
28. Sobolev, A.V., Portnyagin, M.V., Dmitriev, L.V., et al., Petrology of Ultramafic Lavas and Associating Rocks in the Trodos Massif, Cyprus, *Petrologiya*, 1993, vol. 1, no. 4, pp. 379–412.
29. Sobolev, A.V. and Slutskii, A.B., Composition and Conditions of Crystallization of Initial Melt of Siberian Meimechites Related to the General Problem of Ultrabasic Magmas, *Geol. Geofiz.*, 1984, no. 12, pp. 97–110.
30. Tokarev, P.I., *Izverzheniya i seismicheskii rezhim vulkanov Klyuchevskoi gruppy* (Eruptions and Seismic Regime of the Klyuchevskoy Volcanic Group), Moscow: Nauka, 1966.
31. Utnasin, V.K., Anosov, G.I., Balesta, S.I., and Budanskii, Yu.A., Seismic Models of the Klyuchevskoy Volcanic Group in *Zemnaya kora i verkhnyaya mantiya Aziatskoi chasti Tikhookeanskogo kol'tsa* (Earth's Crust and Upper Mantle in the Asiatic Part of the Pacific Ring), Yuzhno-Sakhalinsk, 1975, issue 37, pp. 83–92.
32. Fedotov, S.A., On Input Temperatures of Magmas and Formation, Dimensions, and Evolution of Magma Chambers, *Vulkanol. Seismol.*, 1980, no. 4, pp. 3–29.
33. Fedotov, S.A., Zharinov, N.A., and Gorel'chik, V.I., Deformations and Earthquakes of Klyuchevskoy Volcano: Activity Model, *Vulkanol. Seismol.*, 1988, no. 2, pp. 3–42.
34. Khrenov, A.P., Recent Basaltic Volcanism in Kamchatka, *Doctoral (Geol.–Min.) Dissertation*, Moscow, 2003.
35. Khubunaya, S.A., Bogoyavlenskii, S.O., Novgorodtseva, T.Yu., and Okrugina, A.M., Mineralogical Features of Magnesian Basalts as a Reflection of Fractionation in the Magma Chamber of Klyuchevskoy Volcano, *Vulkanol. Seismol.*, 1993, no. 3, pp. 46–68.
36. Khubunaya, S.A. and Sobolev, A.V., Primary Melts of Calc–Alkaline Magnesian Basalts from Klyuchevskoy Volcano, Kamchatka, *Dokl. Akad. Nauk*, 1998, vol. 360, no. 1, pp. 100–102 [*Dokl.* (Engl. Transl.), 1998, vol. 360, no. 4, pp. 537–539].
37. Aloisi, M., Cocina, O., et al, Seismic Tomography of the Crust underneath the Etna Volcano, Sicily, Phys. Earth Planet. Inter., 2002, vol. 134, pp. 139–155.
38. Churikova, T., Dorendorf, F., and Worner, G., Sources and Fluids in the Mantle Wedge below Kamchatka, Evidence from Across-Arc Geochemical Variation, J. Petrol., 2001, vol. 42, part 8, pp. 1567–1593.
39. Ford, C.E., Russel, D.G., Craven, I.A., and Fisk, M.Q., Olivine-Liquid Equilibria: Temperature, Pressure and Composition Dependence of the Crystal/Liquid Cation Partition Coefficients for Mg, Fe^{2+}, Ca, Mn, *J. Petrol.*, 1983, vol. 24, pp. 256–265.
40. Frezotti, M.L., Silicate-Melt Inclusions in Magmatic Rocks: Applications to Petrology, *Lithosphere,* 2001, vol. 55, pp. 273–299.
41. Danyushevsky, L.V., Green, D.H., Falloon, T.J., and Sobolev, A.V., The Compositions of Anhydrous and H_2O-Undersaturated Melts in Equilibrium with Refractory Peridotites at 15 and 20 kbar: Implications for High-Ca Boninite Petrogenesis, *J. Mineral. Magaz.*, 1994, vol. 58, pp. 209–210.
42. Danyushevsky, L.V., Sobolev, A.V., and Kononkova, N.N., Methods of Studying Magma Inclusions in Minerals during Investigations on Water-Bearing Primitive Mantle Melts (Tonga Trench Boninites), *Geochem. Int.*, 1992, vol. 29, pp. 48–62.
43. Danyushevsky, L.V., McNeill, A.W., and Sobolev. A.V., Experimental and Petrological Studies of Melt Inclusions in Phenocrysts from Mantle-Derived Magmas: An Overviev of Techniques, Advatages and Complications, *Chem. Geol.*, 2002, vol. 183, pp. 5–24.

44. Draver, H.J. and Jonston, R., The Petrology of Picritic Rock in Minor Intrusions - A. Hebridean Group, *Trans. R. Soc. Edinburgh*, 1958, vol. 63, pp. 459–467.

45. De Natale, G., Zollo, A., et al., An Image of Mt. Vesuvius Obtained by 2D Seicmic Tomography, *J. Volcanol. Geotherm. Res.*, 1998, vol. 82, pp. 161–173.

46. Kersting, A.B. and Arculus, R.J., Klyuchevskoy Volcano, Kamchatka, Russia; the Role of High-Flux Recharged, Tapped and Fractionated Magma Chamber (S) in the Genesis of High-A_2O_3 from High-MgO Basalt, *J. Petrol.*, 1994, vol. 35, no. 1, pp. 1–41.

47. Maurel, C. and Maurel, P., Etude Experimentale de Equilibre Fe^{2+} - Fe^{3+} Dans les Spinelles Chroifieres et les Liquides Silicates Basiques Coexistans, a 1 Atm, in Comptes Rendus de L'Academie des Sciences, Paris: 1982, vol. 295, pp. 209–212.

48. Hofmann, A.W., Chemical Differentiation of the Earth: the Relationship between Mantle Continental Crust and Oceanic Crust, *Earth Planet. Sci. Lett.*, 1988, vol. 73, pp. 287–310.

49. Ramsay, W.R.H., Crawford, A.J., and Foden, J.D., Field Setting, Mineralogy, Chemistry and Genesis of Arc Picrites, New Georgia, Solomon Islands, *Contrib. Mineral. Petrol.*, 1984, vol. 88, pp. 386–402.

50. Roedder, E., Fluid Inclusions, *Mineral. Soc. Am.*, 1984, p. 644.

51. Simkin, T. and Smit, J.V., Minor-Element Distribution in Olivine, *J. Geol.*, 1970, vol. 78, no. 3, pp. 304–325.

52. Sisson, T.W. and Layne, G.D., H_2O in Basaltic Andesite Glass Inclusions from 4 Subduction-Related Volcanoes, *Earth Planet. Sci. Lett.*, 1993, vol. 117, nos. 3–4, pp. 619–635.

53. Sobolev, A.V. and Chaussidon, M., H_2O Concentrations in Primary Melts from Island Arcs and Mid-Ocean Ridges: Implications for H_2O Storage and Recycling in the Mantle H_2O Concentrations in Primary Melts from Island Arcs and Mid-Ocean Ridges, *Earth Planet. Sci. Lett.*, 1996, vol. 137, pp. 45–55.

54. Sobolev, A.V. and Danyushevsky, L.V., Petrology and Geochemistry of Boninites from the Termination of the Tonga Trench: Constrains on the Generation Conditions of Primary High-Ca Boninite Magmas, *J. Petrol.*, 1994, vol. 35, pp. 1183–1211.

55. Thompson, A.B., Water in the Earth's Upper Mantle, *Nature*, 1992, vol. 358, pp. 295–302.

56. Touray, J.C., Beny-Bassez, C., Dubessy, J., and Guilhaumou, N., Microcharacterization of Fluid Inclusions in Minerals by Raman Microprobe, *Scan. Electron Microsc.*, 1985, no. 1, p. 103.

57. Wright, T.L. and Doherti, P.C., A Linear Programming and Least Squares Computer Method for Solving Petrologic Mixing Problem, *Geology*, 1970, vol. 81, no. 7, pp. 95–106.

58. Yamamoto, M., Picritic Primary Magma and Its Sourse Mantle for Oshima - Oshima and Bac-Arc Side Volcanoes, Northeast Japan Arc, *Contrib. Mineral. Petrol.*, 1988, vol. 99, pp. 352–359.

59. Zhao, D., Mishra, O.P., and Sanda, R., Influence of Fluids and Magma on Earthquakes: Seismological Evidence, *Phys. Earth Planet. Inter.*, 2002, vol. 132, pp. 249–267.